Intermittent Airblast Atomization and Spray Particle Mixing in Pulsating Air Flow

Young Taig Oh* and Takao Inamura**

(Received Mach 14, 1994)

A new twin-fluid injector applicable to a single-point injector for gasoline engine was developed. Using this injector's transient spray characteristics, the mixing mechanism of spray particles and the deposition mechanism on the inner wall of an intake manifold were investigated. The measurements of spray particle sizes, velocities and deposition rates were experimentally conducted in a pulsating air flow. The particle deposition takes place due to the particle inertia at high air flow rates. At low air flow rates it comes due to the recirculation appearing on the inner wall at the entrance of the intake manifold. On the other hand, the deposition rate of spray particles is strongly influenced by air pulsation. The behavior of spray particle is mainly influenced by air pulsation when the velocity of the atomizing air is low and when the velocity of the air flow around the injector is high. Single small particles follow the air flow more easily than large particles, and this causes the spatial particle size distribution in the spray clump. As the spray particles approach to the tip of a spray clump, the size of particles.

Key words: Airblast Atomization, Single Point Injector(SPI), Gasoline Engine, Twin-fluid Injector, Air Pulsation

Nomenclature

C : number density of spray particles
$\bar{d}_{32}$: Sauter's mean diameter
h : distance from injector to measuring point along center axis of test section
N : rotational speed of butterfly valve
P_o : absolute pressure in test section
q : volumetric flow rate of liquid per stroke
r : radial distance from center axis
R_d: deposition rate of spray particles
t_d : elapsed time since input of fuel injection pulse
t_e : width of the electric injection pulse
V_a: air velocity
V_p: spray particle velocity
W_a: flow rate of air flowing around injector
W_{aa}: flow rate of atomizing air
θ : crank angle
θ_{ph}: injection timing in terms of crank angle

* Department of Mechanical Engineering, Chonbuk National University, Dockjin-Gu, Dockjin Dong Chonju 561-756, KOREA
** Department of Aeronautics and Space Engineering, Tohoku University, Aramaki Aza Aoba, Aoba-ku, Sendai 980, JAPAN

1. Introduction

Electronically controlled fuel injection systems have rapidly come into wide use instead of carburetors. Such an injection system may be classified into two types, namely the single point injection (SPI) system and the multi point injection (MPI) system. As Toyota et al. (1982) mentioned the MPI system can produce high output performances, however, it is disadvantageous from the standpoint of cost. Furthermore, in order to improve fuel economy and exhaust emission characteristics, the lean combustion system has recently been adopted. Takeda et al. (1985) pointed out that in order to achieve a low fuel consumption rate with the lean combustion system and quick transient engine response without sacrificing its cost, a newly developed single point injection system is needed.

Swirl atomizers have been conventionally adopted as the SPI injector, because of their easy handling. Since the swirl atomizer is a pressure-type atomizer, the spray performances become worse rapidly with decreasing fuel pressure. The degradation of this spray performance implies that the fuel consumption rate and exhaust emission characteristics become worse, especially at idling stage.

To improve this fault of the swirl atomizer, various types of atomizers were investigated for the SPI injector. For instance, according to the experimental results obtained by Yamauchi and Nogi (1987), fine spray particles can be easily generated by a twin-fluid atomizer with another air assist method. However, since the velocities of these spray particles are large, particles easily deposit on the inner wall of the intake manifold. Furthermore, it requires an additional air compressor. An ultrasonic atomizer produces spray particles of acceptable sizes with moderate speed and it requires no additional equipment except for an electric circuit. However, it is hard for the ultrasonic atomizer to keep good spray performance over a wide range of fuel flow rates.

Inamura et al. (1986) pointed out that, if the air stream is inhaled by the pressure difference between the vacuum pressure in an intake manifold and the atmospheric pressure and if only the high speed air stream in the intake manifold is available as the atomizing air at a high speed of engine, the fine fuel spray will not be easily obtained without additional equipment over the wide range of driving conditions. In order to achieve the purpose mentioned above, it is necessary to elaborate the design of the injector structure.

The behavior of the fuel spray particles, such as the velocity of each particle, coalescence, disruption and follow up of air velocity in an intake manifold is very important for engine performance and exhaust emissions like the spray characteristics. For example, Nagaishi et al. (1989) made clear experimentally that as the deposition of spray particles becomes worse the fuel consumption rate and transient engine response worsen. In order to decrease the fuel deposition rate, the behavior of fuel spray particles and the deposition mechanism should be clearly explained.

On the other hand, in an intake manifold, the air flow is practically pulsating. The spray formation, spray particle mixing, and deposition on the inner wall are expected to be influenced by the pulsating air flow. Even though Kadota and Kagawa (1987) investigated the particle behavior in a pulsating air flow, there are generally few data available to clarify the deposition mechanism.

This study aims to develop a new single-point injector for gasoline engines which has good spray formation for better engine performances and lower exhaust emissions over a wide range of driving conditions, yet does not need an additional compressor. In the present work, spray characteristics were measured in a pulsating air flow. Furthermore, the mixing mechanism of spray particles in a pulsating air flow was investigated by measuring the spray particle sizes and particle velocities simultaneously using a Phase/Doppler particle analyzer, and the deposition mechanism was investigated by instantaneous photographs and fuel sampling probe.

2. Experimental Apparatus and Instrumentation

As shown in Fig. 1, the experimental apparatus consists of four main components: the air volume measurement component, the spray formation

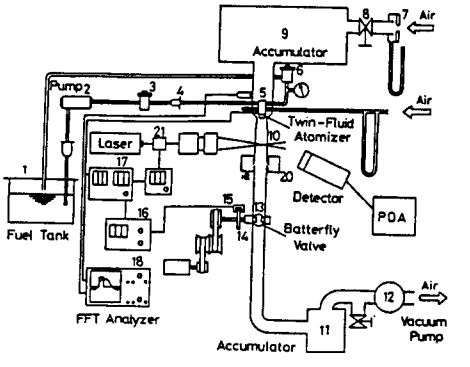

Fig. 1 Experimental apparatus

component, the pulsating air flow formation component and the measurement component. The air volume measurement component consists of a nozzle (7), a throttle valve (8) and an accumulator (9). The spray formation component, inclusive of the twin-fluid atomizer (5), consists of an injector and an intake manifold (10). The pulsating air flow component consists of two butterfly valves (13) and a driven motor (14). The measurement component consists of a Phase/Doppler particle analyzer (16,17,21), a FFT analyzer, a pressure pick-up and two regulators. The liquid in the tank (1) is supplied to the injector (5) by a pump (2) through an accumulator (3) and a filter (4). The injection pressure of the liquid is kept at 100 kPa by a pressure regulator (6). The Mineral Spirit A, whose physical properties are similar to those of gasoline is employed as an alternative fuel. The density of Mineral Spirit A is 798 kg/m^3, its surface tension is 25.0×10^{-3} N/m and its viscosity is 1.43×10^{-3} Pa · s in the condition of 20 ℃ and atmospheric pressure. The air is inhaled by a vacuum pump (12) through the accumulator (9). The air flow rate is measured by an orifice flow meter (7) and the pressure in the test section (10) is adjusted by means of a valve (8). The diameter of the test section, made of Pyrex glass, is 50 mm, in accordance with the intake manifold size of an actual 1500 cc gasoline engine with 4 cylinders. The pulsating air flow is generated by a rotating butterfly valve (13). By changing the rotational speed of the butterfly valve the pulsation frequency can be varied.

Figure 2 shows details of the structure of a newly developed twin-fluid injector. As shown in Fig. 2, the liquid is intermittently injected from eighteen small holes of 0.4 mm in diameter, directed towards the inner wall of the injector. A conical liquid sheet is generated after impingement of the liquid jet to the inner wall, as shown in Fig. 2. The conical liquid sheet is atomized by the high speed air stream flowing around the injector and the air stream inhaled by the pressure difference between the atmospheric pressure and the vacuum pressure in the test section. Hereafter, the air stream flowing around the injector will be known as the "surrounding air stream" and the air stream inhaled by the pressure difference as the "atomizing air stream". The optimum dimensions of the injector were determined based on the theoretical analysis proposed by Inamura et al. (1991) and the results of an experiment carried out by Inamura et al. (1992)

The shape of the entrance of the test section is depicted in Fig. 3. It was designed so that the air velocity becomes maximum at the injector tip for better spray characteristics. This shape may affect the air flow around the entrance. However, according to the preliminary experiments the effects of the entrance shapes on the particle deposition rates were relatively small.

The air velocity in the test section was mea-

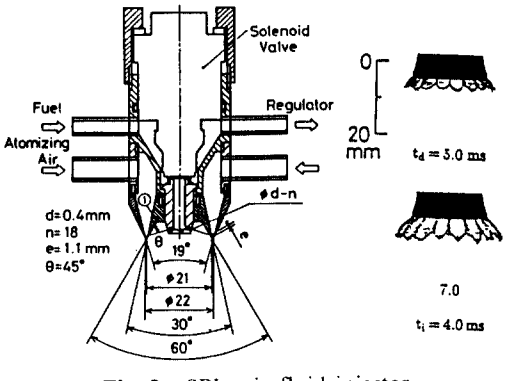

Fig. 2 SPI twin-fluid injector

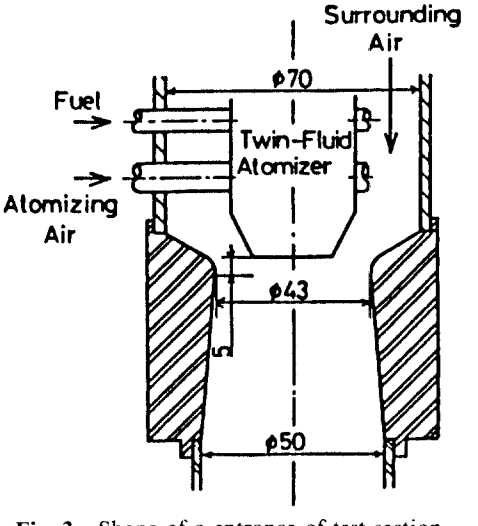

Fig. 3 Shape of a entrance of test section

sured by a hot wire anemometer, and the vacuum pressure was measured by a diaphragm-type pressure transducer. The hot wire was installed 2 mm downstream from the injector, perpendicular to the air flow. Particle sizes, particle velocities and number densities of spray particles were measured simultaneously by a Phase/Doppler particle analyzer (PDPA, DANTEC) with a two Watts Ar-Ion laser. The temporal variations of the particle sizes and particle velocities were measured by the PDPA with an acousto-optic modulator (AOM). The particle deposition rates on the inner wall of the test section were measured by the liquid sampling instrument (20). The injected fuel is separated by two parts, that is, one is the liquid sheet fuel that is flowed onto the inner wall of the intake manifold, the other is the atomization fuel in the intake manifold. The deposition rate is defined as a volume rate of the fuel stock at the inner wall of intake manifold over the whole injected fuel.

In this study the experimental conditions were determined according to the driving conditions of an actual 1500 cc gasoline engine with 4 cylinders. The rotational speed of an actual 4 stroke/4 cylinders engine is equal to that of a butterfly valve. The widths of an electric injection pulse, t_i, were also determined according to driving conditions. Table 1 shows the experimental conditions.

Table 1 Experimental conditions

W_a(g/s)	W_{aa}(g/s)	P_o(kPa)
43.1	2.2	90.8
33.0	2.6	81.3
18.1	3.0	66.7
9.9	3.3	57.9

N=750, 1000, 1500, 2000(rpm)
t_i=2.9, 3.3, 3.7, 4.2(ms)

Figure 4 gives the relation between the volumetric flow rate of liquid per stroke and t_i. The liquid flow rate diminishes at $t_i \cong 0.75$ ms. This means that the opening of a needle valve in the injection takes 0.75 ms. The liquid flow rate is proportional to the substantial injection duration regardless of the injection intervals(or rotational speeds).

3. Results and Discussion

Figure 5 describes the air velocity variations versus the crank angle at 2 mm downstream from the injector. The atomizing air velocity was measured at r=10 mm, and the surrounding air velocity at r=13 mm. At low air flow rates the effects of the crank angle on the air velocity are generally small. In particular, the atomizing air velocity is almost constant against the crank angle, and is much larger than the surrounding air velocity. On the other hand, at a high air flow rate the effects of the crank angle on both air velocities are large, and the atomizing air velocity is almost the same as the surrounding air velocity. This is due to the fact that the air velocity in the test section increases and that the pressure in the test section also increases as the air flow rate increases. The pressure increase in the test section causes the decrease of atomizing air velocity, and the effects of the pulsation on the atomizing air

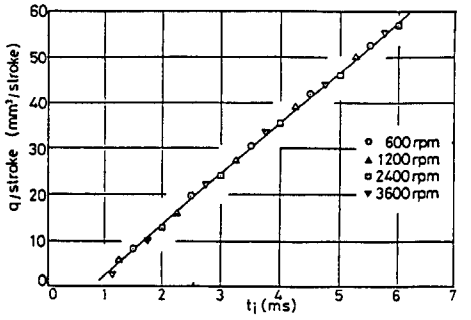

Fig. 4 Relation between liquid flow rate and t_i

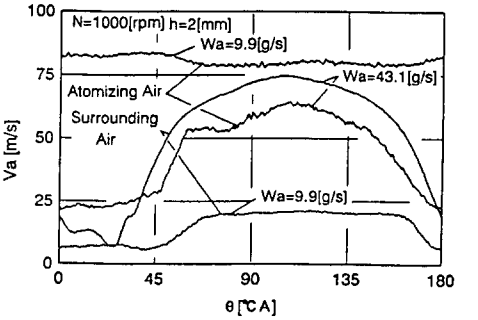

Fig. 5 Variation of air velocity vs. crank angle

velocity becomes large. Since the cross-sectional area of the atomizing air flow in the injector is small, the friction loss is large. Thus, at low air flow rate, namely under low pressure in the test section, the flow rate of the atomizing air is hardly influenced by pressure fluctuations.

The shapes of the fluctuation wave of pulsating air velocity may not be precisely the same as those of practical engines. However, as will be indicated below, the important aspect of the behaviors of spray particles are not exact shapes of the fluctuation wave but the pulsation of air flow itself. Hence, the results obtained in present experiments are applicable to actual engines.

Figure 6 presents the effects of injection timing on the behavior of spray particles. In this condition, the effect of pulsating air flow is very strong, θ_{ph} is larger, and the air velocity of the intake manifold during the injection duration is higher as shown in Fig. 5. In the case of $\theta_{ph}=14.9$ ℃ A, there are large particles in the spray clump; its spray formation is poor because the spray particles are issued from the injector at a low air velocity. Furthermore, if θ_{ph} is larger, since the air velocity of intake manifold is increasing, the recirculation flow is created by the vacuum pressure that is generated below the injector. Therefore, the spray particles have a tendency to gather together toward the center of intake manifold and then broad. In the case where θ_{ph} is the largest (90 ℃ A), the effect of vacuum pressure is the stronger since spray particles are issued from the injector at a high air velocity. Thus, the particles after injection instantly gather toward the center of the intake manifold because the axial velocity

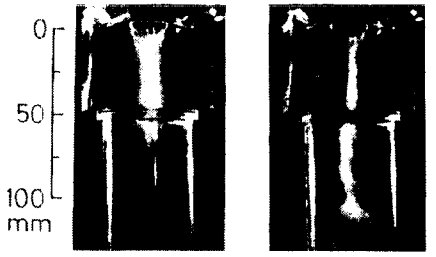

N = 2000 rpm, W_a = 43.1 g/s, t_i = 4.2 ms, t_d = 6.5 ms

Fig. 6 Behavior of spray particles

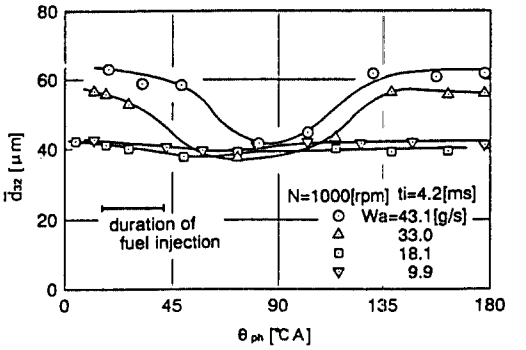

Fig. 7 Variation of $\bar{d}_{32}$ vs. injection timing (N= 1000 rpm)

is larger than the radial velocity, and the spray clump is stretched and becomes narrow.

Figure 7 describes the variation of Sauter's mean diameter $\bar{d}_{32}$ versus injection timing at constant rotational speed, N = 1000 rpm. The symbol ⟷ in Fig. 7 represents a duration of the fuel injection and the other symbols indicate $\bar{d}_{32}$ at the center of the duration. At the small air flow rates (W_a=9.9, 18.1 g/s) the values of $\bar{d}_{32}$ are almost constant against the injection timing. At the large air flow rates (W_a=33.0, 43.1 g/s) the values of $\bar{d}_{32}$ become a minimum at about $\theta_{ph}=70$ ℃ A. As shown in Fig. 5, at small air flow rates the atomizing air velocity is larger than the surrounding air velocity, and then it and its fluctuations become dominant over the spray characteristics. The fluctuations of the atomizing air velocity are small. Therefore, at small air flow rates the mean particle size becomes constant. On the other hand, at larger air flow rates the surrounding air velocity largely affects the spray characteristics, and the maximum value and fluctuation of that becomes large. The air velocity becomes a maximum around $\theta=105$ ℃ A , but the values of $\bar{d}_{32}$ do not exactly become a minimum around it. The fact that the injection timing at a minimum value of $\bar{d}_{32}$ is not coincident precisely with the crank angle at the maximum air velocity indicates that the injection timing at a minimum value of $\bar{d}_{32}$ is probably related to the duration of fuel injection.

Figure 8 describes the variation of $\bar{d}_{32}$ versus injection timing at constant air flow rate, W_a=43.1 g/s. Since the air flow rate is large, the value of

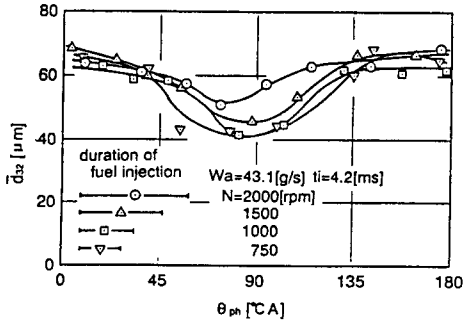

Fig. 8 Variation of $\bar{d}_{32}$ vs. injection timing (W_a=43.1g/s)

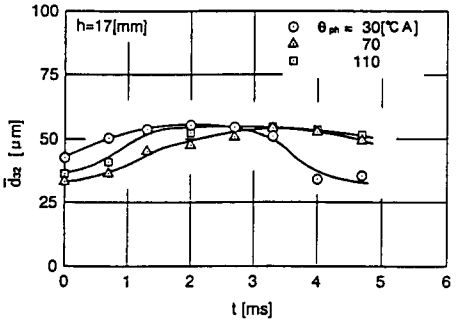

Fig. 9 Variation of $\bar{d}_{32}$ vs. elapsed time (h = 17 mm)

$\bar{d}_{32}$ is greatly influenced by the surrounding air velocity. The reason why $\bar{d}_{32}$ becomes a minimum around θ_{ph}=70 ℃ A was mentioned above. As the rotational speed decreases the variation of $\bar{d}_{32}$ increases. This is due to the fact that, the effects of the air velocity on $\bar{d}_{32}$ increase because the duration of fuel injection decreases as rotational speed decreases as shown by the symbol ⟷ in Fig. 8.

Figure 9 shows the variation of $\bar{d}_{32}$ versus the elapsed time after the tip of the spray clump passing through the measuring volume of PDPA at h=17 mm. The injection duration is 4.2 ms (25.2 ℃ A in terms of crank angle). At θ_{ph}=70 and θ_{ph}=110 ℃ A, the values of $\bar{d}_{32}$ increases as t increases. As shown in Fig. 5, at high air flow rates, the atomizing air velocity and the surrounding air velocity are large and almost constant during the fuel injection. Thus, there is little coalescence and disruption of each of the particles because their scale is large and their fluctuation is low. Therefore, it seems that particle size is almost constant during the fuel injection. Generally, a smaller particle flow along the air stream is more easily accelerated than a larger one because of its smaller inertia. In this case, since the air velocity is larger than the particle velocity, a particle is continuously accelerated until it arrives at the measuring point. Therefore, smaller particles arrive at the measuring point early and the larger particles arrive later.

At θ_{ph}=30 ℃ A the atomizing air velocity and the surrounding air velocity are just increasing during fuel injection as shown in Fig. 5. An increase of the air velocity results in a decrease of the particle size, and it causes a decrease of $\bar{d}_{32}$ for larger t than 4 ms in Fig. 9. And, as shown in Fig. 5, since the air velocity at θ_{ph}=30 ℃ A is smaller than that at θ_{ph}=70, 110 ℃ A during fuel injection, $\bar{d}_{32}$ is larger than those at θ_{ph}=70, 110 ℃ A for smaller t than 3 ms.

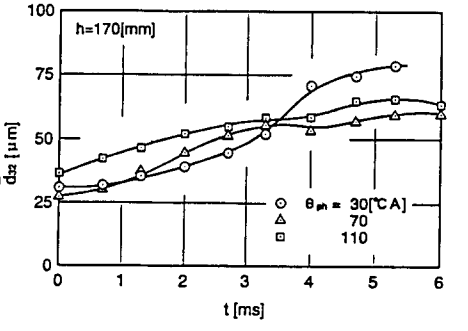

Fig. 10 Variation of $\bar{d}_{32}$ vs. elapsed time (h = 170 mm)

Figure 10 shows the variation of $\bar{d}_{32}$ measured at h=170 mm. The variation of $\bar{d}_{32}$ versus t is larger than that shown in Fig. 9. This is due to the acceleration of particles by the air flow. When t is smaller than 3 ms, the values of $\bar{d}_{32}$ decreases as θ_{ph} decreases. When t is larger than 4 ms, the values of $\bar{d}_{32}$ increases as θ_{ph} decreases. This is because spray particles issued at small θ_{ph} are accelerated more due to the small injection velocities of the particles.

Figure 11 presents the variation of particle density C (number of particles per unit volume) versus elapsed time measured at h=35 mm. As mentioned in the explanation of Fig. 6, a spray clump issued at high air velocity is stretched more

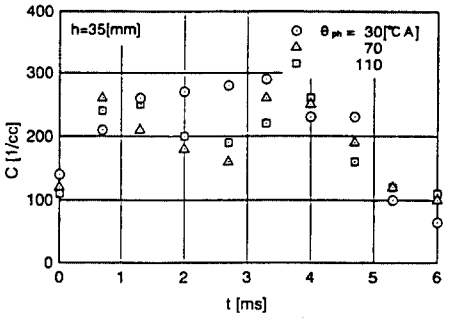

Fig. 11 Variation of C vs. elapsed time (h=35 mm)

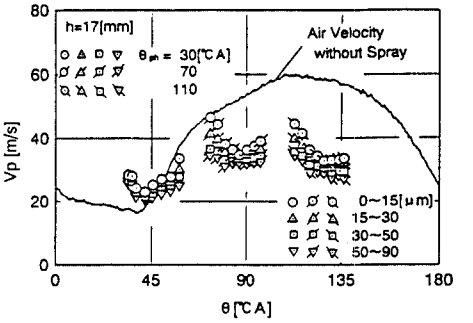

Fig. 12 Variation of V_p vs. crank angle (h=17 mm)

narrowly than that issued at low air velocity. Therefore, the particle density of the spray issued at high air velocity, namely $\theta_{ph}=70$, 110 ℃ A, is generally smaller than that issued at low air velocity, namely $\theta_{ph}=30$ ℃ A. And for all θ_{ph} the particle density first increases and then decreases. This tendency is due to the fact that, fuel flow rate decreases at the beginning and the end of fuel injection.

Figure 12 gives the variation of particle velocity versus crank angle measured at h=17 mm. For all the injection timings the particle velocities have a tendency to decrease first and then increase. Since the particle density increases first and then decreases with increasing crank angle as shown in Fig. 11, particle velocities have reverse tendencies. The velocities of the particles issued at $\theta_{ph}=70$, 110 ℃ A are larger than those issued at $\theta_{ph}=30$ ℃ A. And the velocities of the particles issued in the first half of the fuel injection duration at $\theta_{ph}=30$ ℃ A are larger than the surrounding air velocity. This is due to the fact that, as shown in Fig. 5, in the first half of the fuel injection duration, atomizing air velocity is larger than surrounding air velocity. Since the concentration of particle issued in the first stage of fuel injection duration at $\theta_{ph}=30$ ℃ A is lean, generally each particle flows along the air stream more easily, and then the velocities of particles are the same as the air velocity. It was certified that the velocities of particles in the last stage of the fuel injection rapidly increase according to increase the air velocity in the condition of a downstream from h=35 mm. At the lower downstream, a particle of the first stage is accelerated until it

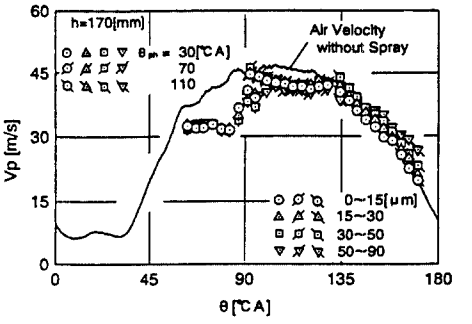

Fig. 13 Variation of V_p vs. crank angle (h=170 mm)

approaches the same value of air velocity. Meanwhile, it is considered that the particles of low velocity in the last stage of the spray were increased because they are easily accelerated due to the low concentration of particles.

Figure 13 shows particle velocities measured at h=170 mm. Since the velocities of particles issued at $\theta_{ph}=70$, 110 ℃ A are almost the same as the air velocity, most of particles flow along the air stream. On the other hand, the velocities of particles issued at $\theta_{ph}=30$ ℃ A are smaller than the air velocity. In this case since the particle velocities at atomization stage are rather small, the particles are not accelerated enough even at h=170 mm. In case of $\theta_{ph}=110$ ℃ A in contrast with $\theta_{ph}=30$ ℃ A, air velocity is decelerating after fuel injection. Therefore, the velocities of particles near the spray tip were large because the air velocity at the beginning was larger than those of the middle and end of spray. However, as particles flow downstream, the velocities of particles approach the air velocity. In addition, large particles were accelerated by air velocity, and they flow along the air

stream, but when the air velocity is decreased near h=170 mm, the velocity of a large particle is larger than the air velocity because of the inertia of the particle.

In order to make clear the relations between the acceleration rate and the particle size, the particle velocity and particle size were measured simultaneously with the various injection timings and with very short fuel injection duration ti=1.4 ms (in terms of crank angle θ=8.4 ℃ A). In this run the atomizing air velocity was decreased in order to generate large particles, too. The results measured at h=70, 135 mm are shown in Fig. 14 and Fig. 15, respectively. At h=70 mm for all particle sizes the particle velocity was smaller than the air velocity. The larger the particle size, the smaller the particle velocity was. These tendencies indicate that all particles go through an acceleration stage.

On the other hand, at h=135 mm the particle velocities are almost the same as the air velocity except the largest particles. Summarizing the results, the small particles easily flow along the air stream while the large particles are hardly accelerated and decelerated. This is because of the differences of particle inertia with different particle sizes. In the range of smaller than 30 ℃ A the velocities of all the particle are larger than the air velocity, but these data are perceived to be in error because of the limitation of velocity range of PDPA. It can be presumed that small particles practically flow along at air velocity.

The deposition of injected fuel on the inner wall of the intake manifold creates a disproportion in the local air-fuel ratio in the combustion chamber and results in poor engine response. Figure 16 and Fig. 17 show the results of the deposition rate.

Figure 16 describes the variations of particle deposition rate R_d versus injection timing at constant rotational speed, N=2000 rpm. As the air flow rate increases the particle deposition rate decreases throughout the injection timing. And R_d shows a minimum at around θ_{ph}=70 ℃ A. According to the observation of spray behavior by the photographs, the larger the air velocity the thinner the spray clump is stretched. This stretch of the spray clump results in low particle deposi-

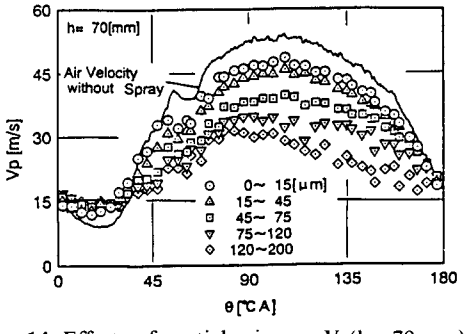

Fig. 14 Effects of particle size on V_p(h=70 mm)

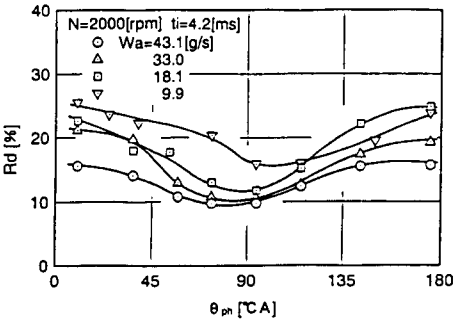

Fig. 16 Variation of R_d vs. injection timing

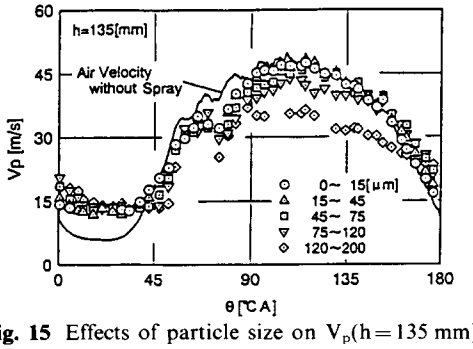

Fig. 15 Effects of particle size on V_p(h=135 mm)

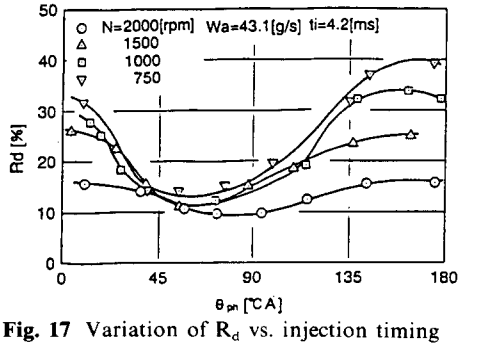

Fig. 17 Variation of R_d vs. injection timing

tion rate. In contrast, at low air flow rates a recirculation zone is formed on the inner wall near the entrance of the test section, and the recirculation tends to promote the deposition of particles on the inner wall.

Figure 17 describes the variations of the particle deposition rate versus injection timing at constant air velocity, W_a=43.1 g/s. R_d has almost the same minimum value at around θ_{ph}= 45 ℃ A against the rotational speed. The lower the rotational speed the larger the variation of R_d. As mentioned above, the particle deposition rate is increased with decreasing air velocity due to recirculation. As a shorter duration of fuel injection is obtained by a lower rotational speed, the influence of the air velocity on the particle deposition rate increases with decreasing rotational speed. Thus, the particle deposition rate at low rotational speeds increases greatly at low air velocity.

In the case of low air flow rates, the recirculation zone was formed because the atomizing air velocity (W_{aa}) is larger than the surrounding air velocity (W_a). In this condition, it is supposed that only a small number of large particles are produced due to high air velocity for atomization. Therefore, most of the deposited fuel is produced by the adhesion of fine particles which is caused by swirl occurring in the recirculation zone around the wall of the intake manifold.

4. Conclusions

A new twin-fluid single point injector was developed for gasoline engines. Using this newly developed injector, spray characteristics and the behavior of spray particles were investigated in the pulsating air flow. The mean particle sizes, particle velocities, number densities and deposition rates of spray particles on the inner wall of the intake manifold were influenced by flowing air pulsation, in particular at high air flow rates. The small particle follows the air flow more easily than the large particle, and this causes the spatial particle size distribution in the spray clump. The spray particles in the vicinity of the tip of a spray clump are smaller than those in the latter half of a spray clump.

A conventional injector requires of high pressure air for atomization and it has been difficult to obtain test results in actual use because of its poor spray in a low air flow rate. However, the newly developed single-point injector has a fine spray over a wide range of operating conditions as well as low air flow rates, and so the results in present experiments are probably applicable to the actual engines.

References

Inamura, T., Nagai, N. and Ikuma, T., 1986, "A Study on the Control of Spray Characteristics of Twin-Fluid Atomizers," *Trans. JSME (Ser. B)*, Vol. 52, No. 476, pp. 1784～1792. (in japanese)

Inamura, T., Nagai, N., Sunanaga, H. and Masubuchi, M., 1991, "The Behavior of a Liquid Film Formed by an Impinging Jet on a Solid Wall (1st Report)," *Trans. JSME (Ser. B)*, Vol. 57, No. 536, pp. 1327～1331. (in Japanese)

Inamura, T., Nagai, N. and Sunanaga, H., 1992, "Improvement for Spray Performance of a Low-Pressure Atomizer by Conical Sheet Formation," *Trans. JSME (Ser. B)*, Vol. 58, No. 551, pp. 2296～2301. (in Japanese)

Kadota, T. and Kagawa, R., 1987, "Behavior of Droplets in Pulsating Air Flow through an Intake Manifold," *Trans. JSME* (Ser. B), Vol. 54, No. 500, pp. 1008～1013.(in Japanese)

Nagaishi, H., Miwa, H., Kawamura, Y. and Saitoh, M., 1989, "An Analysis of Wall Flow and Behavior of Fuel in Induction Systems of Gasoline Engines," *SAE Paper* No. 890837.

Takeda, K.,Shiozawa, K., Oishi, K. and Inoue, T., 1985, "Toyota Central Injection (CI) System for Lean Combustion and High Transient Response," *SAE Paper* No. 851675.

Toyoda, T., Inoue, T. and Aoki, K., 1982, "Single Point Electronic Injection System," *SAE Paper* No. 820902.

Yamauchi, T. and Nogi, T., 1987, "Engine Control System for Lean Combustion," *SAE Paper* No. 870291.